Intensity-dependent quasi-periodic oscillations in the X-ray flux of GX 5-1

van der Klis, M.; Jansen, F.; van Paradijs, J.; Lewin, W.H.G.; van den Heuvel, E.P.J.; Trumper, J.E.; Sztajno, M.

Link to publication

ARTICLES

Intensity-dependent quasi-periodic oscillations in the X-ray flux of GX5-1

M. van der Klis*, F. Jansen†, J. van Paradijs‡, W. H. G. Lewin‖,
E. P. J. van den Heuvel‡, J. E. Trümper¶ & M. Sztajno¶

* Space Science Department of ESA, European Space Research and Technology Centre, Postbus 299, 2200 AG Noordwijk, The Netherlands
† Laboratory for Space Research Leiden, Postbus 9504, 2300 RA Leiden, The Netherlands
‡ Astronomical Institute 'Anton Pannekoek', University of Amsterdam, Roetersstraat 15, 1018 WB Amsterdam, The Netherlands
‖ Massachusetts Institute of Technology, Center for Space Research and Department of Physics, Room 37-627, Cambridge, Massachusetts 02139, USA
¶ Max-Planck Institute for Extraterrestrial Physics, 8046 Garching (b. Munich), FRG

The X-ray flux of the bright galactic bulge source GX5-1 shows intensity-dependent quasi-periodic oscillations between ~20 and ~40 Hz, appearing as a broad peak in the power spectrum whose centroid frequency, width and integrated excess power strongly depend on the source intensity. The strength and steepness of low-frequency noise present in the power spectra below 15 Hz also depend on the source intensity. No evidence is found for coherent X-ray pulsations between 0.5 and 2,000 Hz. We discuss possible mechanisms to explain these new phenomena.

NEUTRON stars in low-mass X-ray binaries have long been suspected to have been spun up to periods in the millisecond range. Several searches for such short rotation periods in low-mass X-ray binaries have been made but none has been successful (refs 1-4 and J. Fleischman, S. Rappaport, D. Strahss and W. Lewin, personal communication). We have renewed the search using the medium energy detectors of the X-ray observatory Exosat. One of the first sources we observed was the bright bulge source GX5-1, in which we found no periodic pulsations but, unexpectedly, we discovered quasi-periodic oscillations. These oscillations are the subject of this report; some preliminary results have already been reported[5].

Observations

We observed GX5-1 (4U 1758–25) with the medium-energy detector[6] (ME) and the gas scintillation proportional counter[7] on Exosat. The observations started on 18 September 1984 11:50 UT and lasted for ~8 h. We shall discuss 1-18-keV data obtained with the Ar/CO₂-filled proportional counters of the medium-energy detector; the counters were co-aligned with a total effective area of 1,500 cm². The data were obtained in 2-s blocks, each containing 8,192 samples (time resolution ~0.25 ms). Within each of the 1,623 blocks, the data are continuous with a negligible 'dead time' of ~1% and between two consecutive data blocks there is a gap of ~15 s. The data contain no spectral information.

Figure 1 shows the counting rate as a function of time. The data include an approximately constant background of ~80 c.p.s. The sharp drop near $r = 17,000$ s is caused by a change ('trim') in the satellite pointing direction. The reason for this trim was the high counting rate, at which detector damage was feared. Before the trim, the collimator efficiency was 93%, whereas afterwards it was 65%.

For the average spectral shape, as measured with the gas scintillation proportional counter, 1 c.p.s. from the ME (pre-trim collimator efficiency) corresponds to $\sim 9.2 \times 10^{-12}$ erg cm⁻² s⁻¹ (1-18 keV), or ~0.3 μJy (2-11 keV). The source flux (~700– ~1,100 μJy) and its variability on a timescale of hours are similar to those encountered previously[8-12]. All count rates described here have been reduced to the pre-trim collimator efficiency.

Analysis and results

To investigate the variability of GX5-1 on timescales between 0.5 ms and 2 s, we estimated the power spectrum by calculating (via a fast Fourier transform (FFT) algorithm) the Fourier amplitudes of the average-subtracted signal in each 2-s block
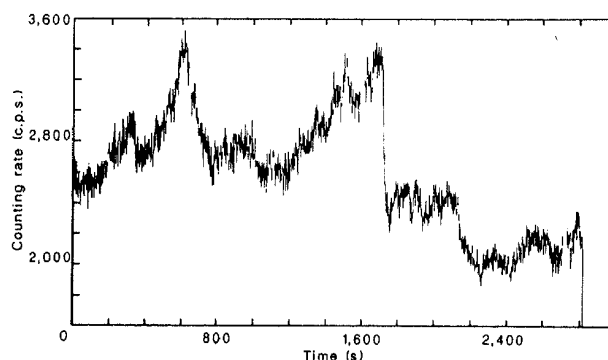

Fig. 1 Average counting rates in 2-s time intervals. Zero time corresponds to 18 September 1984, 11:53:35 UT. The sharp drop near ~17,000 s is the result of a change in the pointing direction of the satellite (see text).

separately. The power spectra of single data blocks are too noisy to allow meaningful study. However, the average of these power spectra clearly shows three components: (1) low-frequency noise below 15 Hz (the power increases towards lower frequencies); (2) a strong broad peak with a centroid frequency near 30 Hz; and (3) a flat spectrum above 100 Hz, consistent with Poisson noise.

No evidence was found for coherent pulsations in the X-ray flux. The 99% confidence upper limit to the pulsed fraction of coherent pulsations in the 50-400-Hz range is 0.3%; in the 400-2,000-Hz range it varies between 0.6 and 2.5%, depending on frequency. In calculating these values, we followed the procedures described by Leahy et al.[3] and took into account possible Doppler shifts resulting from orbital motion of the source and the satellite.

Power density estimates, using conventional FFT techniques, may be in error because of low-frequency 'leakage', if a steep low-frequency ('red') noise component is present[13]. The power-law slope of the red noise in our data is considerably below the critical value of 2, above which problems may occur. Low-frequency leakage is therefore not expected to affect our analysis. This was confirmed by tests on artificial red-noise data and by repeating the analysis of the 2-s blocks after 'detrending' each of them by subtracting a low-order polynomial.

The properties of the broad peak in the power spectrum (centroid frequency, width and integrated excess power) and the low-frequency noise (slope, and integrated excess power) strongly depend on source intensity. In Fig. 2a, b we show the

observed power spectra as a function of time and source intensity, respectively. The broad peaks in the power spectra are seen in Fig. 2a as a dark 'ribbon'; the low-frequency noise is visible at the bottom. The centroid frequency ν_c is clearly correlated with the source intensity (Fig. 2a). Also, both the quasi-periodic oscillations and the low-frequency noise diminish at high source intensity. The dependence of ν_c on source intensity is approximately linear (Fig. 2b). This dependence is not affected by the ~30% drop in counting rate caused by the 'trim' near $t = 17{,}000$ s (Fig. 1). A power-law dependence, however, is also consistent with the data.

The fact that ν_c depends on source intensity and not on the counting rate in the instrument convinced us that the peak in the power spectrum is related to a phenomenon in GX5-1 and is not an instrumental effect or an artefact of the analysis. In this context we mention that background data obtained immediately before and after our observation with the same time resolution, and observations of several other sources of similar brightness, did not show a peak in the power spectrum.

As far as we can tell at this stage of the analysis, all variable properties of the power spectra depend on the source intensity only. To describe the power spectra quantitatively, we performed least-squares-fits to the averages of power spectra selected from six source-intensity intervals. As a fitting function we used

$$P(\nu) = A + B\,e^{-\gamma\nu} + C[(\nu - \nu_c)^2 + (\lambda/2)^2]^{-1} \qquad (1)$$

where P is the power density and B and C are normalization constants. The first term on the right-hand side (a constant) describes the white-noise component. In our adopted normalization[3] one expects $A = 2$ for poissonian noise. The low-frequency noise is well described by an exponential function (second term in equation (1)). A power law does not adequately fit the data.

We used a Lorentz profile with a full-width at half maximum, λ, and centroid frequency ν_c (third term in equation (1)) to describe the peak. We also tried to fit the peak with a gaussian profile; this did not give better power-law fits to the low-frequency data. (The width and integrated excess power of the peak are then 20–30% lower.)

The fits of expression (1) to the averaged power spectra (first 512 frequencies) have a reduced χ^2 between 1.03 and 1.17 for 506 degrees of freedom. The variance of the power estimates was taken as $4/N$, N being the number of power spectra averaged[3]. Examples of the fits are shown in Figs 3 and 4. For decreasing source intensity, ν_c decreases, the peak becomes narrower and the low-frequency noise component steepens.

Figure 5 shows plots of the numerical results (listed in Table 1). The centroid frequency of the peak (Fig. 5a) shows a strong, approximately linear correlation with source intensity. The peak width (Fig. 5b) and the steepness of the low-frequency noise spectrum (Fig. 5c) show an approximately monotonic dependence on the source intensity. The integrated excess power of both the peak (Fig. 5d) and the low-frequency noise (Fig. 5e) show a maximum, roughly halfway in the observed intensity range.

The width and integrated excess power of the peak are 30–50% lower than shown in Fig. 5 (b, d) if we choose a power-law description of the low-frequency noise (both for a lorentzian and a gaussian peak profile). The centroid frequency is very insensitive to changes in the fitting function.

In principle, the broad peaks in the averaged power spectra could result from the averaging out of very narrow peaks which occur at different frequencies in the power spectra of the individual 2-s data blocks. However, the peak remains broad when the data are analysed in intervals as sort as ~100 s.

We shall assume that the averaged power spectra are representative of those of the individual 2-s blocks. The results can then be interpreted as resulting from a signal that shows quasi-periodic oscillations of which the typical period decreases from 50 to 25 ms and the coherence time (defined as the e folding time of autocorrelation function) from 75 to 25 ms when the source intensity increases by ~30%. The signal also contains low-frequency noise to which the contribution of slower vari-
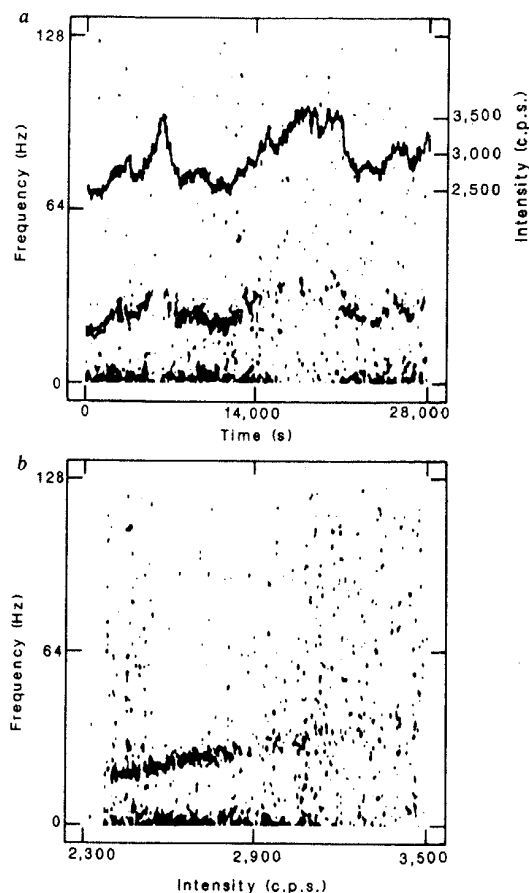

Fig. 2 a, Display of the temporal variation of the power spectra. The frequency is in the vertical direction (left-hand scale). A vertical cross-section of the display is a grey-scale coded representation of a power spectrum. The darker the shade the higher the power it represents. To conserve the quality of the picture, the original display of 512×512 pixels has been smoothed with a gaussian profile with $\sigma = 1.3$ pixels. The variable broad peak in the power spectra is visible as a dark 'ribbon'; the low-frequency noise is visible at the bottom. Also shown is the intensity of GX5-1 (right-hand scale). The peak frequency depends strongly on source intensity. Also, notice that both the quasi-periodic oscillations and the low-frequency noise diminish at high source intensity. b, Display (see a) of the power spectra as a function of source intensity (reduced to pre-trim collimator efficiency). The peak frequency is approximately linearly related to source intensity.

ations becomes weaker for increasing source intensity and of which the strength (integrated excess power) depends on the source intensity in a way very similar to that of the peak.

The noise process that underlies the quasi-periodic character of these oscillations is not strongly constrained by our present analysis; the counting rates are too low to allow us to follow individual wave trains. It could be the result of (see, for example, ref. 14): (1) a superposition of randomly excited damped harmonic oscillators; (2) random phase variations of a periodic wave train; (3) the superposition of closely spaced periodic oscillations whose frequencies are distributed over a finite interval. It is also conceivable that the broad peak is the result of a dependence of the peak frequency on the X-ray photon energy, which is smeared out because of the absence of energy resolution in our data.

Discussion

Intensity-dependent quasi-periodic oscillations, such as those reported here, have not been observed previously (millisecond X-ray oscillations lasting of the order of 10 s have been reported[2,15] which are probably unrelated). The variations in frequency of the oscillations clearly exclude the possibility that
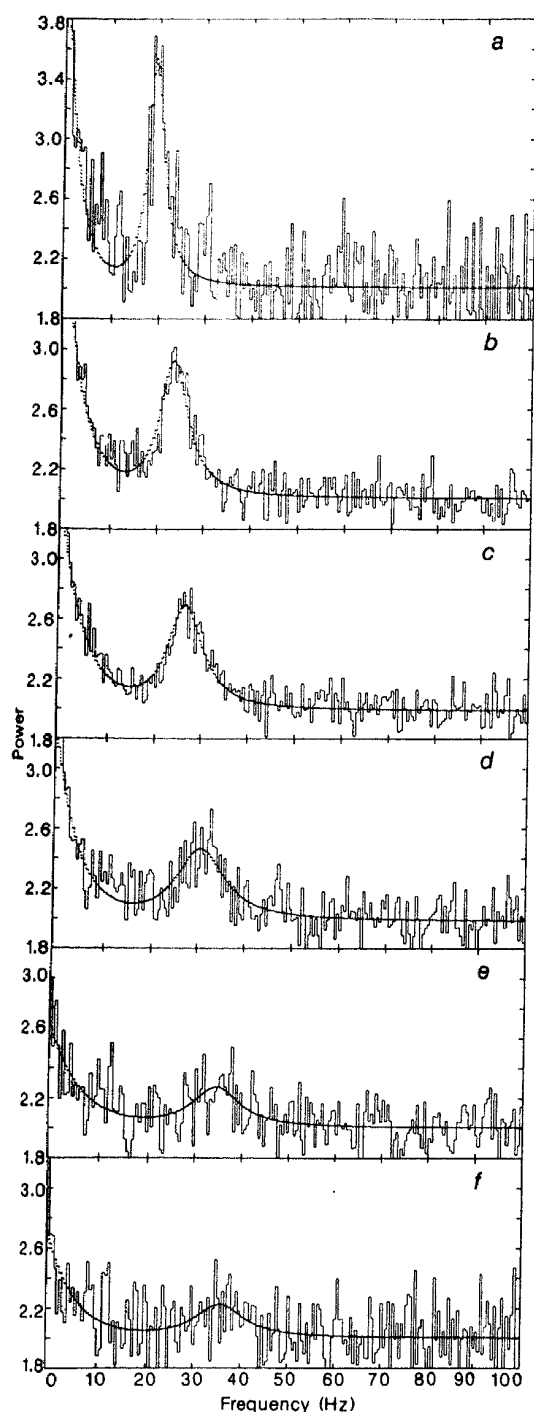
Fig. 3 Linear displays of average power spectra of GX5-1 in six different source-intensity intervals. a, 2,277-2,486; b, 2,486-2,695; c, 2,695-2,904; d, 2,904-3,113; e, 3,113-3,322; f, 3,322-3,531 (c.p.s.). The average has been taken over the power spectra of individual 2-s intervals (see text). Fits of equation (1) to the data are also shown. Notice the change of centroid frequency and width of the peak as a function of source intensity.

they represent the rotation period of the compact object.

Quasi-periodic oscillations on timescales of the order of tens of seconds are a common phenomenon in cataclysmic variables[14,16,17]. Of particular interest are the optical oscillations seen during some dwarf-nova outbursts which show a positive correlation between frequency and (optical) flux[14,18,19]. Apart from the $\sim 10^3$ times longer period and the different energy band, these oscillations differ from those in GX5-1 by: (1) the generally one to three orders of magnitude larger coherence; (2) the

positive correlation between coherence time and source intensity[19] (negative in GX5-1, see Figs 3, 4, 5b); and (3) the much weaker dependence of frequency on optical flux.

Models proposed for these dwarf-nova oscillations include inhomogeneities rotating with the inner accretion disk[20,21], or with the white dwarf envelope[22]; disk oscillations[23,24]; oscillations in the atmosphere of the white dwarf[25,26]; and various instabilities in the accretion flow (for example 27-29; for reviews see refs 14, 18). We examine some of these models in the context of our new findings for GX5-1, assuming that the compact object is a neutron star; in the case of cataclysmic variables the compact object is a white dwarf.

The dependence of the frequency of the oscillations on the source intensity in GX5-1 is strong ($d \log \nu_c / d \log I \sim 2$). The accretion-flow instability models of Langer[28] and Livio[29] can be excluded on this ground alone. The model of King[22], which involves magnetic loops anchored in a differentially rotating envelope of the compact object, predicts the correct sense for the correlation of intensity with frequency and coherence of the oscillations, but does not make quantitative predictions.

Non-radial g- or r-mode oscillations of the neutron star envelope could have periods in the range observed by us[30,31]. Proposed excitation mechanisms for these oscillations are thermonuclear flashes[32] (see also ref. 33) and sudden accretion events[34]. However, X-ray bursts have never been observed from GX5-1. It is unclear whether, with a mass-accretion rate varying by $\sim 30\%$, the second mechanism can be considered viable.

In Bath's[20] model for dwarf-nova oscillations, the oscillations originate from inhomogeneously distributed matter ('blobs') orbiting the compact object with the Kepler frequency at some preferred radius, in particular that of the magnetosphere, r_m. In the case of spherical accretion, r_m is given by[35,36]

$$r_m = (2.9 \ 10^8 \ \text{cm}) \ \mu_{30}^{4/7} \ m^{1/7} \ R_6^{-2/7} \ L_{37}^{-2/7} \qquad (2)$$

Here μ_{30} is the magnetic moment of the compact object in units of 10^{30}G cm^3, m its mass in units of solar masses, R_6 its radius in units of 10^6 cm and L_{37} the X-ray luminosity in units of 10^{37} erg s^{-1}. In our further discussion we assume $m = R_6 = 1$.

The keplerian frequency ν_K at the magnetospheric radius depends on the X-ray luminosity according to

$$\nu_K = (0.37 \ \text{Hz}) \ L_{37}^{3/7} \ \mu_{30}^{-6/7} \qquad (3)$$

With $\nu_K \sim 30$ Hz and $L_{37} \sim 10$, one infers $\mu_{30} \sim 2 \times 10^{-2}$ or, equivalently, a surface magnetic field strength $B_0 \sim 2 \times 10^{10}$ G and $r_m \sim 160$ km. The relation between the frequency of the quasi-periodic oscillations and the luminosity for GX5-1 is qualitatively as predicted by equation (3). However, as mentioned above, the observed value for the exponent is about five times the predicted value of $3/7$, and this may indicate that this model[20] is not applicable here. Alternatively, disk oscillations[23,24] could occur near, for example, the magnetospheric radius. The periods of disk oscillations are of the order of the Kepler periods[37]; the oscillations would then occur at a radius of $\sim 10^2$ km. The quasi-periodic oscillations in the X-ray flux could, for example, be produced by intermittent occultations of the X-ray source by the orbiting blobs or by the oscillating disk.

Warner[21] suggested that the observed frequency, ν_c, of the dwarf nova oscillations is the beat frequency of the (keplerian) disk frequency, ν_k, at the magnetospheric radius and the rotation frequency, ν_s, of the white dwarf. Alphar and Shaham[38,39] suggest the same idea to explain the oscillations in GX5-1. For the case of the neutron star this leads to

$$\nu_c = (0.37 \ \text{Hz}) \mu_{30}^{-6/7} \ L_{37}^{3/7} - \nu_s \qquad (4)$$

The dependence of ν_c on luminosity can then be made stronger at will by a proper choice of the value of ν_s. A fit of relation (4) to our data (dashed curve in Fig. 5a) yields $(\nu_s)^{-1} = 10.5 \pm 0.4$ ms and $B_0 = (6.3 \pm 0.3) \times 10^9$ $(D/10$ kpc) G; here D is the source distance. The magnetospheric radius is ~ 60 km.

The derived magnetic field strength depends strongly on whether the blobs are seen at the magnetospheric radius, r_m (equation (2)), or at some other radius. According to Ghosh and Lamb[40], for disk accretion, the appropriate magnetospheric

radius is $\sim 0.5 \times r_m$, which would lead to a field three times stronger. However, the above value for ν_s would not change.

A potential problem with models involving a magnetosphere[20,21,38,39] is the absence in our data of coherent X-ray pulsations, resulting from the neutron star's rotation, with a period near 10 ms (see Fig. 4). The upper limit (99% confidence level) to the pulsed fraction of coherent pulsations with periods in the range from 5 to 20 ms is 0.3%. Compared with a 'classical' X-ray pulsar, for example, HerX-1 ($B_0 \sim 4 \times 10^{12}$ G; ref. 41), the magnetospheric properties of GX5-1 would be very different. The magnetospheric radius would be ~ 50 times smaller, the magnetic dipole field at r_m $\sim 10^2$ times higher, the opening angle of the accretion column near the magnetic pole a factor of ~ 6 larger, the density of the inflowing matter at $r_m \sim 3 \times 10^3$ times larger and the column density outside the magnetosphere $\sim 10^2$ times larger. It is therefore possible that the neutron star in GX5-1 cannot be seen directly because it is obscured by plasma. It is also conceivable that a special geometry of 'X-ray beams' may hide the signature of the neutron star spin, or that the magnetic and rotation axes are co-aligned.

Despite the fact that the beat-frequency model[21,38,39] has been introduced in a rather ad-hoc fashion to account for the observed relation between frequency and intensity, the inferred rotation period and magnetic-field strength of the neutron star fit well[38] into an existing evolutionary framework for the galactic bulge sources[42,43], which links these objects to the 6-ms radio pulsar[44] PSR1953 + 29.

In this evolutionary model[42,43], neutron stars in bright galactic bulge sources are spun up to millisecond rotation periods because of accretion from an evolved companion, and the X-ray
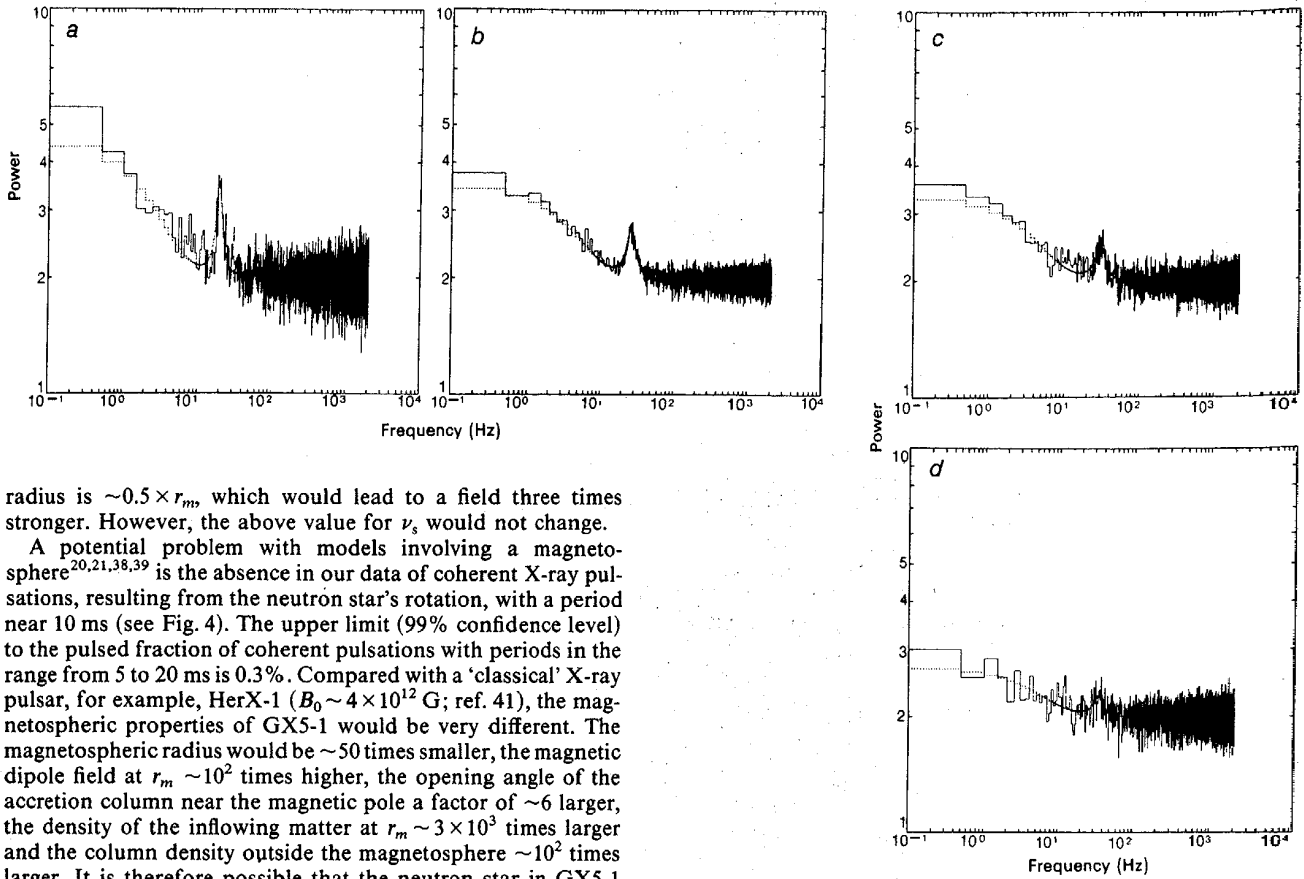
Fig. 4 Logarithmic displays of average power spectra in four different source intensity intervals (see Fig. 3 legend). a, 2,277–2,486; b, 2,695–2,904; c, 2,904–3,113; d, 3,113–3,322 (c.p.s.). The dependence of the low-frequency noise on source intensity is seen more clearly than in Fig. 3.

sources evolve into wide binary radio pulsars[45-47]. (That a spun-up neutron star with a relatively weak magnetic field, in a binary, may later on show up as a fast radio pulsar was first suggested by Smarr and Blandford[48] and further elucidated in refs 49-53.) The rotation period of ~ 10 ms, as predicted by the beat-frequency model for GX5-1, is in accordance with the evolutionary model[42,43]. The magnetic dipole field strength of PSR1953 + 29 ($\leq 2 \times 10^{10}$ G; refs 45, 54) is comparable to that predicted by

Table 1 Best-fit parameters of power spectra

N	97	425	464	288	208	128
I_{lim} (c.p.s.)	2,277–2,486	2,486–2,695	2,695–2,904	2,904–3,113	3,113–3,322	3,322–3,531
$\bar{I}$ (c.p.s.)	2,427	2,603	2,790	3,001	3,225	3,403
ν_c (Hz)	20.07 ± 0.15	24.38 ± 0.16	27.26 ± 0.2	31.25 ± 0.5	35.11 ± 1.0	36.35 ± 1.6
λ (Hz)	4.2 ± 0.6	7.6 ± 0.5	9.2 ± 0.7	12.6 ± 2.0	12.4 ± 4.0	12.6 ± 10.0
P_{peak} (10^4 (c.p.s.)^2)	2.47 ± 0.13	2.89 ± 0.13	3.27 ± 0.2	3.33 ± 0.4	2.03 ± 0.6	2.02 ± 1.0
f_{peak} (%)	6.48 ± 0.17	6.53 ± 0.15	6.48 ± 0.2	6.08 ± 0.4	4.42 ± 0.7	4.18 ± 1.0
γ (s)	0.367 ± 0.04	0.247 ± 0.014	0.211 ± 0.014	0.216 ± 0.02	0.168 ± 0.04	0.188 ± 0.08
P_{LFN} (10^4 (c/s)^2)	2.32 ± 0.15	2.65 ± 0.10	2.83 ± 0.12	2.72 ± 0.19	1.93 ± 0.25	2.15 ± 0.4
f_{LFN} (%)	6.28 ± 0.2	6.25 ± 0.12	6.03 ± 0.13	5.50 ± 0.19	4.31 ± 0.3	4.31 ± 0.4
A	2.011 ± 0.009	2.004 ± 0.004	1.987 ± 0.004	1.983 ± 0.005	2.003 ± 0.007	2.002 ± 0.010
χ^2_ν (506 d.f.)	1.17	1.07	1.03	1.09	1.07	1.05

Results of least-squares fits of equation (1) to averaged power spectra taken from six source-intensity intervals. N is the number of individual power spectra (2-s data blocks) averaged, the values for I_{lim} indicate the limits in source intensity defining the intervals, and $\bar{I}$ is the average intensity within each interval. Peak centroid frequency ν_c, full-width at half-maximum λ, steepness parameter γ of the low-frequency noise and the white-noise level A are defined by equation (1). P_{peak} and P_{LFN} are the integrated excess power in the peak and in the low-frequency noise, respectively. These numbers are the integrals ($\nu = 0$ to ∞) of the third and the second term, respectively, of the fits of equation (1), to the power spectra, normalized to assign a power a^2 to a sinusoidal modulation with amplitude a. f_{peak} and f_{LFN} are the corresponding relative amplitudes. Quoted errors correspond to the extreme limits of the $\chi^2_{min} + 1$ error contours.

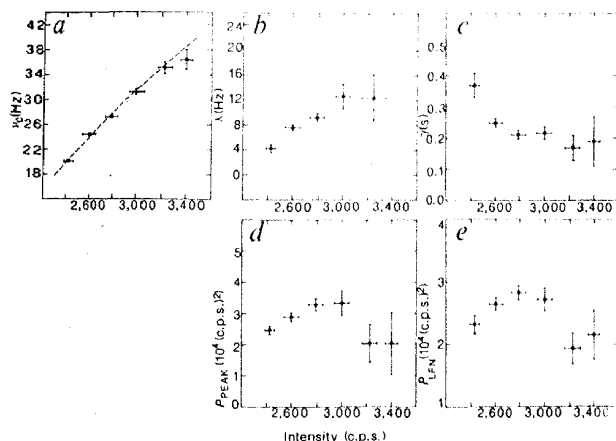**Fig. 5** Parameters of the power spectra (see Table 1) as a function of source intensity. *a*, Centroid frequency ν_c of the peak in the power spectrum. The dashed curve is a fit of equation (4) to the points. Clearly, a linear relation would also be an excellent fit to our results. *b*, Full-width at half maximum, λ, of the peak in the power spectrum. In this panel the two highest intensity intervals have been combined. *c*, Steepness parameter, γ, of the low-frequency noise. *d*, Integrated excess power of the peak in the power spectrum. Note the striking similarity with *e*. *e*, Integrated excess power of the low-frequency noise. Note the striking similarity with *d*. Vertical error bars are 1σ single-parameter, and take correlations between parameters in the fit into account. Horizontal bars represent the standard deviations of the intensity distributions in each of the six chosen intervals.

the beat-frequency model for the neutron star in GX5-1. These coincidences make the beat-frequency model attractive, but they could well be accidental.

Magnetic fields of neutron stars probably decay on a timescale of $(2-5) \times 10^6 \, yr^{[55]}$ (but see ref. 56). Therefore, if the quasi-periodic oscillations in GX5-1 are related to a magnetosphere (with a magnetic field strength of the neutron star of the order of 10^{10} G), the age of the neutron star in GX5-1 is probably of the order of 5×10^7 yr. Van den Heuvel and Taam[57] pointed out that, in the above evolutionary model[42,43], neutron stars are most probably formed during the mass-transfer phase by the accretion-induced collapse of a white dwarf. The mass-transfer phase in systems with an evolved companion lasts only $\sim 10^8$ yr. Thus, neutron stars in such systems could be relatively young ($< 10^8$ yr). The mass-transfer phase in systems with low-mass unevolved companions can last up to $\sim 10^9$ yr. Thus in those systems the probability of finding a relatively young neutron star is small. Therefore, if magnetospheric models are correct and the above evolutionary scenario is applicable, one would expect that similar quasi-periodic oscillations in low-mass X-ray binaries may be observed preferentially in systems which have an evolved companion star.

Our data suggest that the low-frequency noise is a different manifestation of the same phenomenon that causes the oscillations (notice the similarity between Fig. 5*d* and *e*). If we speculate that the X-ray oscillations are the result of 'blobs' in the inner accretion disk, the low-frequency noise could perhaps represent the size distribution of the blobs, larger blobs contributing to the noise power at lower frequencies. The blobs would have to disappear when the source intensity is high (decline of low-frequency noise). In this scenario, we can derive a lifetime for the blobs of 0.1–0.2 s from the observed width of the peaks in the power spectra. This estimate is based on the assumption that during its lifetime a blob causes a wavetrain of constant amplitude and frequency. We observe (see Fig. 5*b*, *c*) that when the steepness of the low-frequency noise is at a maximum (many large blobs present), the peak in the power spectrum is relatively narrow (long blob lifetime). This is contrary to what would be expected if this lifetime is dictated by differential keplerian rotation[58].

Possibly there is a 'gating' mechanism which allows incoming blobs (producing the low-frequency noise) to accrete in a piecemeal fashion (producing the quasi-periodic oscillations). This mechanism could then 'exhaust' the blobs, and now larger blobs may survive longer than smaller ones, consistent with our observations. A gating mechanism would probably fit in any of the above magnetospheric models[20,21,38].

Clearly, the scenarios and ideas discussed here are speculative. Any successful model must produce a physical mechanism explaining the observed properties of the quasi-periodic oscillations and the low-frequency noise, including their strong dependence on the source intensity.

We observed GX5-1 again for ~ 8 h on 29 April 1985. An analysis, performed the same day, showed that the quasi-periodic oscillations were again present. When this manuscript was in the final stage of typing, Dr W. Priedhorsky and his co-workers informed us that they observed (personal communication) similar phenomena from ScoX-1 as described here for GX5-1.

Note added in proof: Models for the quasi-periodic oscillations along the lines suggested at the end of this article have been proposed by Alpar, Lamb and Shaham[59] and by Berman and Stollman[60]. Intensity-dependent quasi-periodic oscillations have also been detected in CygX-2 (Hasinger *et al.*, IAU Circ. 4070), and quasi-oscillations have been demonstrated to be intensity dependent in ScoX-1 (M.v.d.K. *et al.*, IAU Circ. 4068). We point out that CygX-2 has an evolved companion, which supports our suggestion that the oscillations will be preferentially observed in such systems. We thank Fred Lamb for a useful discussion concerning the coherence time of the oscillations.

1. Lewin, W. H. G. in *Advances in Space Exploration* (eds Baity, W. A. & Peterson, L. E.) 133-149 (Pergamon, Oxford, 1979).
2. Sadeh, D. *et al. Astrophys. J.* 257, 214-224 (1982).
3. Leahy, D. A. *et al. Astrophys. J.* 266, 160-170 (1983).
4. Langmeier, A., Sztajno, M. & Trümper, J. *Adv. Space Res.* 5, 121-123 (1985).
5. van der Klis, M. *et al. IAU Circ.* No. 4043 (1985).
6. Turner, M. J. L., Smith. A. & Zimmermann, H. U. *Space Sci. Rev.* 30, 513-524 (1981).
7. Peacock, A. *et al. Space Sci. Rev.* 30, 525-534 (1981).
8. Bradt, H. V. D. & McClintock, J. E. A. *Rev. astr. Astrophys.* 21, 13-66 (1983).
9. Davison, P. J. N. *Nature phys. Sci.* 246, 90-92 (1973).
10. Van der Klis, M. & Rappaport, S. *Astr. Astrophys.* 121, 119-123 (1983).
11. Ponman, T. *Mon. Not. R. astr. Soc.* 201, 769-799 (1982).
12. Kendziorra, E., Collmar, W., Brunner, H., Staubert, R. & Pietsch, W. *Proc. 18th ESLAB Symp.*, Scheveningen (Reidel, Dordrecht, 1985).
13. Deeter, J. E. *Astrophys. J.* 281, 482-491 (1984).
14. Cordova, F. A. & Mason, K. O. in *Accretion-driven Stellar X-ray Sources* (eds Lewin, W. H. G. & van den Heuvel, E. P. J.) 147-187 (Cambridge University Press, 1983).
15. Sadeh, D. & Livio, M. *Astrophys. J.* 258, 770-775 (1982).
16. Cordova, F. A., Chester, T. J., Mason, K. O., Kahn, S. M. & Garmire, G. P. *Astrophys. J.* 278, 739-753 (1984).
17. Van der Woerd, H. *et al. Astr. Astrophys.* (submitted).
18. Patterson, J. *Astrophys. J. Suppl.* 45, 517-539 (1981).
19. Hildebrandt, R. H., Spillar, E. J. & Stiening, R. F. *Astrophys. J.* 243, 223-227 (1981).
20. Bath, G. T. *Nature phys. Sci.* 246, 84-87 (1973).
21. Warner, B. in *Cataclysmic Variables and Related Objects* (eds Livio, M. & Shaviv, G.) 155-172 (Reidel, Dordrecht, 1983).
22. King, A. R. *Nature* 313, 291-292 (1985).
23. Robinson, E. L. & Nather, R. E. *Astrophys. J. Suppl.* 39, 461-480 (1979).
24. Van Horn, H. M., Wesemael, F. & Winget, D. E. *Astrophys. J. Lett.* 235, L143-147 (1980).
25. Papaloizou, J. & Pringle, J. E. *Mon. Not. R. astr. Soc.* 182, 423-442 (1978).
26. Papaloizou, J. C. & Pringle, J. E. *Mon. Not. R. astr. Soc.* 190, 43-53 (1980).
27. Cordova, F. A., Chester, T. J., Tuohy, I. R. & Garmire, G. P. *Astrophys. J.* 235, 163-176 (1980).
28. Langer, S. H., Chanmugan, G. & Shaviv, G. *Astrophys. J. Lett.* 245, L23-26 (1981).
29. Livio, M. *Astr. Astrophys.* 141, L4-6 (1984).
30. McDermott, P. N., Van Horn, H. M. & Scholl, J. F. *Astrophys. J.* 268, 837-848 (1983).
31. Livio, M. & Bath, G. T. *Astr. Astrophys.* 116, 286-292 (1982).
32. Van Horn, H. M., McDermott, P. N. & Carroll, B. W. *Conf. Pulsations in Classical and Cataclysmic Variables at JILA* (Boulder, Colorado, 1984).
33. Yahel, R. Z., Brinkmann, W. & Braun, A. *Astr. Astrophys.* 139, 359-367 (1984).
34. Starrfield, S., Kenyon, S., Sparks, W. M. & Truran, J. W. *Astrophys. J.* 258, 683-695 (1982).
35. Davidson, K. & Ostriker, J. P. *Astrophys. J.* 179, 585-598 (1973).
36. Lamb, F. K., Pethick, C. J. & Pines, D. *Astrophys. J.* 184, 271-289 (1973).

37. Pringle, J. E. *A Rev. Astr. Astrophys.* 19, 137-162 (1981).
38. Alpar, M. A. & Shaham, J. *IAU Circ.* No. 4046 (1985).
39. Alpar, M. A. & Shaham, J. *Nature* (in the press).
40. Ghosh, P. & Lamb, F. K. *Astrophys. J.* 234, 296-316 (1979).
41. Trümper, J. *et al. Astrophys. J. Lett.* 219, L105-110 (1978).
42. Webbink, R. F., Rappaport, S. A. & Savonije, G. J. *Astrophys. J.* 270, 678-693 (1983).
43. Taam, R. E. *Astrophys. J.* 270, 694-699 (1983).
44. Boriakoff, V., Buccheri, R. & Fauci, F. *Nature* 304, 417-419 (1983).
45. Joss, P. C. & Rappaport, S. A. *Nature* 304, 419-421 (1983).
46. Paczynski, B. *Nature* 304, 421-422 (1983).
47. Savonije, G. J. *Nature* 304, 422-423 (1983).
48. Smarr, L. L. & Blandford, R. D. *Astrophys. J.* 207, 574-588 (1976).

49. Van den Heuvel, E. P. J. *IAU Symp.* 95, 379-396 (1981).
50. Radhakrishnan, V. *IAU Asian-Pacific Regional Meeting*, Bandung (ed. Hydayat, B.) (1981).
51. Srinivasan, G. & Van den Heuvel, E. P. J. *Astr. Astrophys.* 108, 143-147 (1982).
52. Alpar, M. A., Cheng, A. F., Ruderman, M. A. & Shaham, J. *Nature* 300, 728-730 (1982).
53. Radhakrishnan, V. & Srinivasan, G. M. *Curr. Sci.* 51, 1096-1102 (1982).
54. Helfand, D. J., Ruderman, M. A. & Shaham, J. *Nature* 304, 423-425 (1983).
55. Lyne, A. G. *IAU Symp.* 95, 423-436 (1981).
56. Kundt, W., Özel, M. E. & Ercan, E. N. *Astr. Astrophys.* (preprint).
57. Van den Heuvel, E. P. J. & Taam, R. E. *Nature* 309, 235-237 (1984).
58. Bath, G. T., Evans, W. D. & Papaloizou, J. *Mon. Not. R. astr. Soc.* 167, 7-9P (1974).
59. Alpar, M. A., Lamb, F. K. & Shaham, J. *Astr. Astrophys.* (preprint).
60. Berman, N. & Stollman, G. *Astr. Astrophys.* (preprint).

How the geomagnetic field vector reverses polarity

Michel Prévot*, Edward A. Mankinen†, C. Sherman Grommé† & Robert S. Coe‡

* Laboratoire de Géomagnétisme, CNRS and Université de Paris 6, 94107 Saint-Maur Cédex; Centre Géologique et Géophysique, CNRS and Université des Sciences et Techniques, 34060 Montpellier Cédex, France
† US Geological Survey, Menlo Park, California 94025, USA
‡ Earth Sciences Board, University of California, Santa Cruz, California 95064, USA

A highly detailed record of both the direction and intensity of the Earth's magnetic field as it reverses has been obtained from a Miocene volcanic sequence. The transitional field is low in intensity and is typically non-axisymmetric. Geomagnetic impulses corresponding to astonishingly high rates of change of the field sometimes occur, suggesting that liquid velocity within the Earth's core increases during geomagnetic reversals.

THE Steens Mountain (Oregon) reversed-to-normal polarity transition[1] is probably the most detailed record of a reversal of the geomagnetic field reported from a volcanic sequence. This Miocene reversal occurred 15.5 ± 0.3 Myr ago[2,3] and can be correlated with the older boundary of marine magnetic anomaly 5 B2 (ref. 4). We have completed an extensive palaeomagnetic study of the Steens Mountain reversal to obtain a precise, detailed description of fluctuations in absolute palaeointensity of the geomagnetic field as it reverses. In the course of this study, we also obtained a more complete description of the directional changes during this reversal. These directional and palaeointensity data place new major constraints on the reversing Earth's dynamo.

Field and laboratory methods

We collected slightly over 1,000 oriented samples from three almost completely sampled sections, A, B and C, of the upper two-thirds of the Steens Basalt. Sections A and B are located only 1 km apart on Steens Mountain ($42.63°$ N, $241.43°$ E) and are readily correlated by matching the transitional field directions. Taken together, these two sections span the end of the pre-transitional reversed period, the transition and the post-transitional normal period. Samples from section C ($42.18°$ N, $240.07°$ E), located 130 km to the south-west of Steens Mountain, are reversed with the exception of those from the top flow, which display a transitional direction also observed on Steens Mountain[1] at the start of the reversal. The main eruptive centre was probably close to Steens Mountain, and the reversed part of Section C is believed to be older than the reversed zones sampled at the bottom of sections A and B, on the basis of the sequence of palaeomagnetic directions. The composite section obtained by combining sections A, B and C is 615 m thick and consists of $\sim$120 distinct lava flows, which are numbered within each section from the top to the bottom.

The palaeodirection of the field was calculated from the remanence direction after either alternating field or thermal cleaning. After grouping successive flows with the same average direction of remanence, the Steens record consists of 55 directional groups (also numbered from the top to the bottom) of which 12 are reversed, 29 are transitional and 14 are normal (Fig. 1).

The absolute palaeointensity of the field was determined using the method of Thellier and Thellier[5]. Although time-consuming,

this method is preferable because it relies on experimentally well-established physical laws and a sound theoretical background. In addition, the method allows palaeointensities to be determined without the direct heating of samples to high temperatures required by other methods, which usually result in major magnetochemical changes. We selected 185 samples for palaeointensity investigations with low viscosity index, high Curie point and reversibility (or near-reversibility) of the strong-field magnetization curve versus temperature. These criteria proved to be pertinent. We obtained 157 useable palaeointensity values corresponding to 51 vectorial groups (group of successive flows with the same directions and palaeointensities).

Vectorial description

The transitional state of the geomagnetic field vector may be defined as corresponding to successive vectors of which either the directions or intensities (or both) are outside the range of secular variation observed in the adjacent pre- or post-transitional periods. Using this criterion, the end of the transition corresponds to directional group (DG) 15 whose direction and intensity are both transitional (Fig. 2). The beginning of the reversal was recorded by DG 43, which displays the first transitional palaeointensity (Fig. 2). However, the direction of the field at the same time was only 27° away from that of the reversed dipole (Fig. 1) and may be considered to be within the range of secular variation. Thus, transitional palaeointensities seem to have shortly preceded the transitional directions, which were recorded by the immediately following directional groups. In contrast, normal directions and intensities were recovered simultaneously at the end of the reversal.

Records of secular variation before and after the reversal were used to obtain a crude estimate of the duration of the transition. We assumed that these records are essentially complete because of the high extrusion rate needed to record the field reversal in such detail. A review of archaeomagnetic results[6] shows that the angular rate of change of the virtual geomagnetic pole, when calculated from 2,000 yr BP to the present, is almost the same ($6 \pm 1°$ per 100 yr) for areas as widely separated as Europe, North America and Japan. Assuming that this rate can be used for the Miocene, we found that the reversed and normal records in the Steens Basalt correspond to periods of 5,000 and 3,500 years, respectively. The corresponding accumulation rates of flows at Steens Mountain (sections A and B) are the same (43 ± 4 m per